Effect of Dehydration on Light-Induced Reactions in Photosystem II: Photoreactions of Cytochrome b559[†]

Olga Kaminskaya,[‡] Gernot Renger,*[,§] and Vladimir A. Shuvalov[‡]

Institute of Basic Biological Problems, Russian Academy of Sciences, Pushchino, Moscow Region 142292, Russia, and Max-Volmer-Institute for Biophysical Chemistry and Biochemistry, Technical University Berlin, Strasse des 17, Juni 135, D-10623 Berlin, Germany

Received September 30, 2002; Revised Manuscript Received April 14, 2003

ABSTRACT: The effect of dehydration on the reaction pattern of photosystem II (PS II) has been studied by measuring and analyzing spectral changes induced by continuous wavelength illumination in films of untreated and hydroxylamine-washed PS II membrane fragments dehydrated to different levels. The obtained data revealed (i) the extent of light-induced formation of about one $Q_A^{-\bullet}$ per 230 chlorophylls (Chl) remains virtually invariant to dehydration down to the lowest values of relative humidity (6−8% RH); (ii) a decrease of the RH to 30% leads to severe blockage of the electron transfer from $Q_A^{-\bullet}$ to Q_B and the progressive replacement of water oxidation by photooxidation of high potential (HP) cytochrome (Cyt) b559 in untreated PS II samples or accessory Chl and carotenoid (Car) molecules in samples with preoxidized Cyt b559; (iii) photooxidation of Cyt b559 is followed by its photoreduction, concomitant with photooxidation of Chl and Car; (iv) in dry samples with preoxidized Cyt b559, not more than a half of total Cyt b559 can be photochemically reduced, independent of the extent of Cyt b559 in the HP form; (v) at low RH values, Cyt b559 photoreduction in samples with preoxidized heme groups and photoaccumulation of $Q_A^{-\bullet}$ take place with biphasic kinetics with similar rate constants for both processes; (vi) Cyt b559 photoreduction in dry samples is DCMU insensitive, while the dark rereduction of photooxidized Cyt b559 is inhibited by DCMU; (vii) fast and slow kinetic phases of Cyt b559 photoreduction dramatically differ in their dependencies on the intensity of CW illumination and are associated with electron donation to Cyt b559 from $Q_A^{-\bullet}$ and pheophytin$^{-\bullet}$, respectively. The pathways of light-induced electron transfer in PS II involving Cyt b559 are discussed.

The key steps of photosynthetic water oxidation take place in a multimeric protein complex referred to as PS II[1] that is anisotropically embedded into the thylakoid membrane and enzymatically functions as light-driven water−plastoquinone oxidoreductase. The overall process comprises three types of reaction sequences: (i) light-induced generation of the sufficiently stabilized radical ion pair $P680^{+\bullet}Q_A^{-\bullet}$ (*1*, *2*), (ii) formation of plastoquinol from the quinone via a sequence of two one electron steps with $Q_A^{-\bullet}$ as reductant (*3*, *4*), and (iii) oxidation of two water molecules to molecular oxygen and four protons at a manganese-containing WOC through a four step sequence with $P680^{+\bullet}$ as oxidant and tyrosine Y_Z of polypeptide D1 acting as redox active mediator (*5*−*7*). All cofactors participating in these reaction sequences are bound to a heterodimeric protein matrix consisting of polypeptides D1 and D2. Recent X-ray crystallographic studies have elucidated the spatial arrangement of these cofactors (*8*, *9*). The static structure is an indispensable prerequisite to address questions on the mechanism of electron transfer in biological systems, but a deeper understanding requires information on nuclear dynamics. This most important interplay between protein dynamics and reactivity has been thoroughly analyzed by the pioneering work of Frauenfelder and colleagues for ligand binding to heme proteins (*10*−*12*).

Numerous studies have shown that the reaction sequences i−iii in PS II exhibit quite different dependencies on a degree of protein flexibility. One very illustrative reflection of this striking feature is the characteristic temperature dependencies: the light-induced charge separation takes place at cryogenic temperatures (*13*) down to the level of liquid helium (*14*) whereas sequences ii and iii are thermally blocked below certain threshold temperatures (*15*, *16*) that depend on the redox states of Q_B (*17*) and of the WOC (*18*−*20*). The role of the protein flexibility is nicely illustrated for reaction centers from anoxygenic purple bacteria where X-ray crystallography revealed that the electron transfer from $Q_A^{-\bullet}$ to Q_B leads to a shift of the headgroup of the latter by about 5 Å together with its rotation by nearly 180° around

[†] The support by grants from DFG (436 Rus 113/635/0-1), the Russian Fund of Basic Research (01-04-48752), and INTAS (00-0404) is gratefully acknowledged.

* To whom correspondence should be addressed. Tel: ++49 30 314 22794. Fax: ++49 30 314 21122. E-mail: renger@pc-109ws.chem.tu-berlin.de.

[‡] Russian Academy of Sciences.

[§] Technical University Berlin.

[1] Abbreviations: PS II, photosystem II; Cyt, cytochrome; WOC, water oxidizing complex; Chl, chlorophyll; RH, relative humidity; E_m, midpoint potential; HP, high potential; IP, intermediate potential; LP, low potential; CW, continuous wavelength; PFD, photon flux density; MES, 2-(*N*-morpholino)ethanesulfonic acid; HEPES, *N*-(2-hydroxyethyl)piperazine-*N*′-(2-ethanesulfonic acid); CHES, 2-(*N*-cyclohexylamino)ethanesulfonic acid; FTIR, Fourier transform infrared; Pheo, pheophytin; Car, carotenoid.

10.1021/bi020606v CCC: $25.00
Published on Web 06/18/2003

the isoprenoid side chain (*21*). Although these data prove that the position of Q_B can be drastically shifted, it is not yet clear whether this is the only structural change that limits the $Q_A^{-\bullet}$ reoxidation rate by Q_B (*22*). In PS II, the analogous reaction was also shown to be intimately coupled with protein flexibility (*23*) but detailed structural information as in the case of purple bacteria is still lacking.

Another way to restrict the protein dynamics is to diminish the water activity in biological samples. The latter can be achieved by either dehydration or suspension of proteins in high osmotic media, organic solvents, or incorporation in reversed micelles. In these "low water systems" proteins exhibit high conformational rigidity because the transitions between conformational substates and "breathing" modes are highly restricted because of hindered medium reorganization (*24*−*27*). This gives rise to effects similar to those observed by "freezing" protein modes at low temperatures. It has to be emphasized that the features observed strongly depend on the mode of samples freezing and dehydration. Rapid freezing and sharp decrease of water activity give rise to the locking of proteins in a set of conformational substates. As a consequence, a distribution of rate constants emerges thus leading to complex kinetics of the ensemble for a unimolecular reaction as illustrated for the recombination reaction between $P^{+\bullet}$ and $Q_A^{-\bullet}$ in samples of bacterial reaction centers rapidly frozen (*28*) or dehydrated by trehalose addition (*29*). On the other hand, sufficiently slow freezing or dehydration close to equilibrium conditions leads to protein ensembles in well-defined conformational states. Therefore, in the present study, the latter type of sample treatment was used.

The effect of dehydration has been analyzed under well-defined conditions of water activity in samples of anoxygenic purple bacteria. It was shown that in dehydrated samples the electron transfer from Q_A to Q_B is impaired (*30*, *31*) and the rate of recombination between $P^{+\bullet}$ and $Q_A^{-\bullet}$ is several-fold increased (*30*). Likewise, the extent of photooxidation of membrane-bound Cyt c becomes diminished (*32*). These changes of electron transfer processes correlate with altered conformational dynamics of the reaction center protein (*33*−*35*).

Less detailed information is available for PS II. So far, the effect of dehydration was mainly studied in plant leaves in order to analyze consequences of drought stress by using noninvasive fluorescence techniques and the method of thermoluminescence (see ref *36* and references therein). However, it is difficult to draw sound conclusions on the specific modulation of the PS II reaction pattern because in dissicated plant tissue the extent of thylakoid membrane hydration is not well-defined. Despite these problems, it can be inferred that drying leads to impairment in PS II of both WOC function and plastoquinol formation. It was found that in whole leaves exposed to water stress of different durations photooxidation of Cyt b559 takes place (*37*). This effect can be expected as a consequence of inhibition of the WOC. Recently, a first detailed report was presented on dehydration effects on the WOC in PS II complexes from the thermophilic cyanobacterium *Thermosynechococcus elongatus* (*38*). Using FTIR spectroscopy, it was convincingly shown that the oxidation steps of the WOC are progressively blocked when the water content of the sample decreases. The extent of this effect depends on the redox state S_i of the WOC (*38*). It therefore appears worth analyzing in more detail the effects of dehydration on the reaction pattern of PS II, especially the turnover of redox active components on the donor side that is normally dominated by the physiological function of water oxidation in the WOC.

With respect to redox components of PS II other than P680, Q_A, Q_B, Y_Z, and the WOC, the heme protein Cyt b559 is of special interest. Cyt b559 is an integral constituent of the PS II core complex (*39*−*41*) that intimately interacts with the heterodimeric protein matrix consisting of polypeptides D1 and D2 and carrying all cofactors of photosynthetic water cleavage. The protein matrix of the heme group of Cyt b559 is built by two polypeptides (α- and β-subunit) each containing a single His residue acting as an axial ligand of the heme iron center (*42*−*47*). Cyt b559 is unique among the b-type cytochromes by the existence of a form with an unusually high midpoint potential of +380 to +400 mV (HP form). Several treatments are known that transform the HP Cyt b559 into forms with lower E_m values. Typical redox titrations of PS II membrane fragments with a functionally competent WOC indicate the existence of three forms with distinctly different redox potentials (*48*−*51*). The functional role of Cyt b559 is not yet clarified, but it seems most likely that it is involved in protective reactions to deletereous light stress responses especially after de novo synthesis of PS II complexes without intact WOC (*52*−*59*).

One of the most important problems in understanding the function of Cyt b559 is related to the long standing controversy on the question of whether PS II contains only one or two Cyt b559 heme groups. This problem originates from discrepancies of estimations based on spectrophotometric measurements, especially because of uncertainties of the correct differential extinction coefficient (see Discussion). It is now widely assumed that recent X-ray crystallographic structure analyses have unambiguously answered all questions on the stoichiometry of Cyt b559. PS II complexes isolated from thermophilic cyanobacteria contain only one heme group that is located in the membrane spanning region of the complex toward the stromal side in closer proximity to Q_B than to Q_A (*8*, *9*). X-ray structure data of sufficient resolution are so far lacking for PS II complexes from higher plants. Therefore, at present, the possibility of a different Cyt b559 content in thermophilic cyanobacteria and higher plants cannot be entirely ruled out. However, the situation is even more puzzling because recent proteomics analyses claimed that two Cyt b559 were found in PS II from both mesophilic and thermophilic cyanobacteria (*60*, *61*). As a consequence, the dogma of only one Cyt b559 in all PS II complexes needs unambiguous proof (see Discussion).

The present study describes the results of thorough investigations on the photoaccumulation of $Q_A^{-\bullet}$ and the light-induced redox reactions of Cyt b559 in films of PS II membrane fragments that are dehydrated to well-defined levels by using suitable conditions. The data obtained reveal that the water content of PS II membrane fragments does not affect the light-induced charge separation but seriously impairs both the reduction of Q_B by $Q_A^{-\bullet}$ and the reactions of the WOC thus giving rise to redox turnover of Cyt b559 and the oxidation of Chl and Car. Attempts are made to explain the data within the framework of the "one Cyt b559"

dogma, but a better interpretation is achieved by the assumption of two Cyt b559.

MATERIALS AND METHODS

PS II membrane fragments were obtained from spinach and sugar beet according to the method of Berthold et al. (*62*) with some modifications (*63*). All assays were performed in a buffer containing 50 mM MES (pH 6.5), 0.4 M sucrose, 15 mM NaCl, and 10 mM $CaCl_2$ (standard medium).

Hydroxylamine-treated PS II membranes were obtained by using the procedure described in ref *64* with modifications (*65*). Samples were incubated in a buffer containing 50 mM MES (pH 6.5), 0.4 M sucrose, 15 mM NaCl, 1 mM $CaCl_2$, 1 mM ascorbate, and 5 mM hydroxylamine hydrochloride for 1 h in the darkness at 4 °C and a Chl concentration of 0.5 mg/mL. To check that the content of HP Cyt b559 did not drastically decrease after hydroxylamine treatment, redox titration of heme b559 in the treated PS II membranes was performed as described earlier (*51*). Typically, the distribution of heme b559 redox forms was observed as follows: 388 ± 11 mV (55 ± 3%), 233 ± 15 mV (29 ± 4%), and 100 ± 17 mV (16 ± 3%). These values are similar to those of untreated oxygen-evolving PS II membranes (*48*−*51*) and well agree with data reported earlier for hydroxylamine-treated PS II membranes (*49*). Untreated PS II membrane fragments exhibited typical average oxygen evolution rates under saturating CW light of around 600 μmol of O_2 (mg of Chl)$^{-1}$ h^{-1}, measured at pH 6.5 with 0.5 mM 2,6-dichloro-1.4-benzoquinone and 1 mM $K_3[Fe(CN)_6]$ as acceptors. After hydroxylamine treatment, the rate of oxygen evolution in PS II membrane samples did not exceed 10 μmol of O_2 (mg of Chl)$^{-1}$ h^{-1}.

Dehydration was performed at room temperature on thick films of PS II membrane fragments, which were deposited on a quartz slide fixed in a sealed glass cell, adapted for circulation of a constant flow of air. The RH of the flushing air was measured in the output flow in a constructed chamber equipped with a digital hygrometer. Accuracy of RH measurements was ±3%. PS II membrane films were incubated in the dark for 10 min and then dried to 6−8% RH by air that had passed through $CaCl_2$. Higher RH levels were achieved by a subsequent film rehydration with air equilibrated with saturated salt solutions (*66*). After attaining a constant RH value (typically after 1 h), the cell was hermetically sealed. For each measurement at different RH, a new sample was used.

Optical measurements were performed at room temperature in a Cary 5 spectrophotometer with an optical slit width of 2 nm. Light minus dark difference spectra were recorded between 520 and 590 nm with a scan time of 30 s or between 370 and 720 nm with a scan time of 90 s. The Cyt b559 and $Q_A^{-\bullet}$ concentrations in suspensions of PS II membrane fragments were determined by measuring reduced minus oxidized spectra and using extinction coefficients of 17.5 mM^{-1} cm^{-1} at "560 minus 573 nm" (*39*, *44*) and 3.5 mM^{-1} cm^{-1} at "542 minus 550 nm" (*67*, *68*) for Cyt b559 and C550, respectively. The amplitudes of the signals were determined relative to a straight line connecting the points at 546 and 573 nm (*51*). The Chl concentration of suspensions of PS II membrane fragments was determined according to the method described in ref *69*.

The average number of Chls per PS II was obtained by measurements of the flash-induced oxygen yield under repetitive excitation as outlined in ref *70*. The values of 230 ± 20 obtained for samples with full oxygen-evolving capacity are in excellent agreement with most reports in the literature (*71*−*74*). The total amount of Cyt b559 in PS II membrane fragments was determined by anaerobic redox−titration of the heme group through monitoring of its α-band (*51*). For rapid estimation of the concentration of the HP form of Cyt b559 in a sample, the absorbance increase at 560 nm was measured after addition of 20 mM $K_4[Fe(CN)_6]$ to the sample preincubated with 0.2 mM $K_3[Fe(CN)_6]$. On the basis of the widely used difference extinction coefficient of Cyt b559 reported in refs *39* and *44*, both oxygen-evolving and hydroxylamine-treated PS II membrane preparations were calculated to contain approximately 1.8 Cyt b559 per 230 Chl, with 55−65% and 50−55% of Cyt b559 present in the HP form (initially reduced in the dark) in oxygen-evolving and hydroxylamine-treated PS II membranes, respectively.

The amplitudes of the redox changes of heme b559 and $Q_A^{-\bullet}$ due to illumination or dark incubation of dehydrated samples of PS II membrane fragments were presented as fractions of their 100% levels in buffer suspensions of the same optical density at "623 minus 750 nm" assuming a 10% higher scattering at 623 nm for sample suspensions.

The amplitude of the C550 signal in cases of concomitant changes of the Cyt b559 α-band at 560 nm in the light-induced difference absorption spectra was determined by the following procedure. A normalized reduced minus oxidized difference absorption spectrum of Cyt b559 in the 520−590 nm region obtained in D1−D2−Cyt b559 preparations (see Figure 5A in ref *51*) was added or subtracted, respectively, to (from) the corresponding light-induced difference spectra of Cyt b559 photooxidation or photoreduction recorded in PS II membrane samples.

Chemical oxidation of HP Cyt b559 was performed by incubation of the samples at 4 °C for 15 min in standard buffer medium containing in addition 2 mM $K_3[Fe(CN)_6]$, followed by two wash steps in the same buffer but without the oxidant. All manipulations were done in almost darkness to avoid Cyt b559 photoreduction. After this treatment, the samples retained 50% of Cyt b559 in the HP form, and about 90% of this HP Cyt b559 was in the oxidized state.

For conversion of the HP into the LP form of Cyt b559, oxygen-evolving PS II membrane fragments were incubated at room temperature for 15 min in a medium containing 25 mM CHES (pH 9.16), 0.4 M sucrose, 15 mM NaCl, 10 mM $CaCl_2$, and 0.5 mM $K_3[Fe(CN)_6]$. The pH of this suspension was subsequently shifted back to pH 6.5 by the addition of 150 mM MES buffer. Finally, the sample was washed twice in a standard buffer medium. After this treatment, all Cyt b559 of the sample was in its oxidized LP form.

CW illumination was performed with a 150 W halogen projector equipped with a 600 nm cutoff filter at the PFDs given in figure legends. Kinetic curves were analyzed by a nonlinear curve-fitting Origin program.

RESULTS

On the basis of a difference extinction coefficient at 560 nm of 17.5 mM^{-1} cm^{-1} (*39*, *44*), stoichiometric ratios

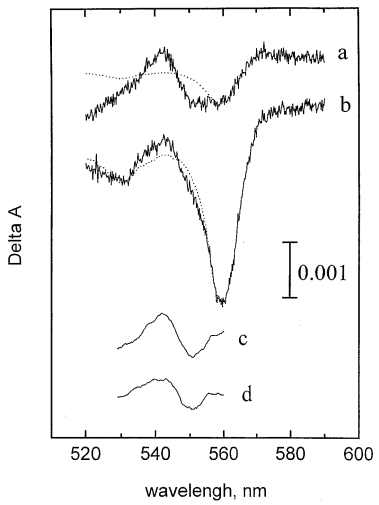

FIGURE 1: Light-induced difference spectra of "wet" (trace a) and "dry" (trace b) films prepared with oxygen-evolving PS II membrane fragments. Films of PS II membrane suspended in standard buffer were dehydrated to a RH of 8% ("dry film") and then rehydrated back to 81% RH ("wet film") as indicated in the Materials and Methods. Spectra were monitored before and after 10 s of actinic illumination with red light; PFD 2200 μEm^{-2} s^{-1}. Optical density of the samples at 623 minus 750 nm was 0.81 A. Two measurements were averaged for each curve. Dotted lines represent the oxidized minus reduced difference spectrum of Cyt b559 normalized to the peak at 560 nm (for details, see the Materials and Methods). Curves c and d represent the difference between experimental data and dotted curves for samples a and b, respectively. Smoothing of curves c and d was done in the Origin program.

of about 1.8 Cyt b559 per PS II were obtained for the membrane fragments used in the present study (see Materials and Methods). However, to avoid confusions because of a possible significant underestimation of this difference extinction coefficient (G. Brudvig, personal communication), in the following description, all data for the light-induced reactions of Cyt b559 will be presented in relative units, i.e., as a percentage of the total content.

As described in the Materials and Methods, about 60% of the total Cyt b559 was initially reduced in oxygen-evolving dark-adapted PS II membrane fragments. The photoinduced signals in samples dehydrated to different extents were measured in the absence of exogenous electron donors or acceptors. Figure 1 shows typical difference absorption spectra in the wavelength region of 520−590 nm induced by 10 s of illumination with saturating CW light in hydrated (a) and dry (here, and later in the text, dry defines samples dehydrated to ≤30% RH) (b) films prepared from oxygen-evolving PS II membrane fragments. Curves a and b of Figure 1 reveal that illumination of both samples gives rise to spectral changes that are the composite of two types of signals. One of these is characterized by bleaching bands at 560 and 532 nm that reflect oxidation of Cyt b559 while the other component with typical features of an electrochromic bandshift around 546 nm is indicative of C550 formation. The latter was clearly resolved by subtraction of a "pure" difference spectrum of Cyt b559 oxidation normalized to the peak at 560 nm (dotted curve) from the light-induced spectra a and b (see Materials and Methods). The remaining contribution shown by the curves c and d, respectively, represents a difference spectrum that is characterized by a trough at 550 nm and a peak at 542 nm and an isosbestic point at 546 nm, which, in good agreement with the previous papers, corresponds to the C550 signal (*68*, *75*−*78*). The latter indicates $Q_A^{-\bullet}$ formation due to the electrochromic effect on Pheo (*75*, *76*).

A comparison of the separated contributions c and d with the experimental difference spectra a and b in Figure 1 readily shows that the amplitude of the C550 signal is smaller but the extent of photooxidized Cyt b559 is much higher in the dry as compared to the wet film. The amplitudes of the C550 signals, gathered from curves c and d, correspond with a photoreduction of 0.79 and 0.53 $Q_A^{-\bullet}$ per 230 Chl, respectively. Correspondingly, the amplitudes of Cyt b559 oxidation in curves a and b of Figure 1 reflect redox changes in 7 and 29% of total Cyt b559, respectively. In marked contrast, analogous experiments carried out in buffer suspension of oxygen-evolving PS II membrane fragments did not lead to any Cyt b559 oxidation upon illumination, in agreement with previous findings (*39*, *56*, *79*). Instead, a very small but reproducible Cyt b559 photoreduction was observed that usually did not exceed 5% of Cyt b559 population. The latter probably reflects a small fraction of reaction centers with HP Cyt b559 initially oxidized.

For the relevance of the above-mentioned findings, it is most important to note that the dehydration effect is largely reversible. This is already illustrated in Figure 1 because the sample used for measuring curve a was obtained by rehydration of a dried film of PS II membrane fragments.

The results of Figure 1 can be explained by the general conclusion that normal redox reactions of PS II are reversibly modified upon dehydration of PS II membrane fragments, but the process of light-induced charge separation is still functioning. Under these conditions, Cyt b559 oxidation is observed, which indicates that the WOC function is impaired. On the basis of the data of Figure 1, it can be concluded that in dry samples of PS II membrane fragments only about 30% of the PS II complexes are transformed into state $Cytb559^{ox}Q_A^{-\bullet}$ by illumination. Therefore, in the following experiments, we tried to find out whether the decrease of the C550 signal upon drying of the sample originates from inhibition of a primary electron transfer in a fraction of PS II complexes or is caused by other effects.

The data in Figure 2 present the kinetics of $Q_A^{-\bullet}$ photoaccumulation in dry films of two different types of PS II membrane fragments that are either fully competent in oxygen evolution (curve a) or deprived of this function by high pH pretreatment (curve b). In the latter sample type also, all HP Cyt b559 is transformed into the LP form as outlined in the Materials and Methods. In the case of oxygen-evolving PS II preparations, data were also collected in the presense of 40 μM DCMU added to the sample before dehydration (filled squares). For each point in Figure 2, a photoinduced difference spectrum analogous to that shown in Figure 1 as trace b was recorded after a definite illumination time given in the abscissa and the pure C550 component was then extracted by subtraction of Cyt b559 redox difference spectrum as described in the Materials and Methods.

Several interesting features emerge from the data of Figure 2: (i) regardless of the WOC integrity, more then 80% of $Q_A^{-\bullet}$ can be photoaccumulated in dried PS II membrane fragments; (ii) PS II membrane fragments with an intact WOC exhibit biphasic kinetics of $Q_A^{-\bullet}$ formation (curve a in

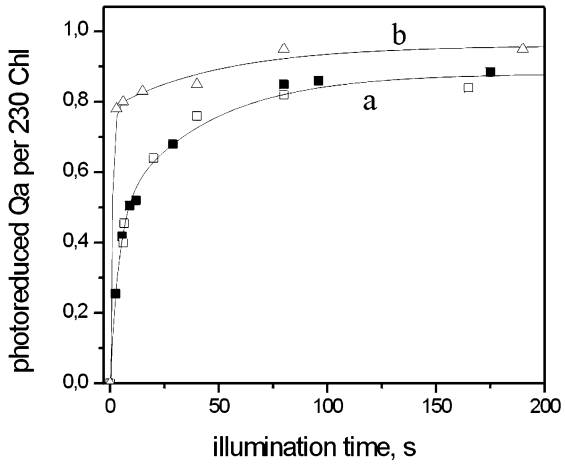

FIGURE 2: Normalized extent of $Q_A^{-\bullet}$ formation as a function of illumination time in dry films of untreated and high pH-treated PS II membrane fragments. Films prepared from oxygen-evolving (squares) and high pH-treated (triangles) preparations of PS II membranes were dehydrated to 8% RH. Filled squares show the experiment where 40 μM DCMU was added to suspensions of oxygen-evolving PS II membranes before film preparation. Full line curves represent biexponential fitting of the experimental data: amplitude factors $a_1 = 0.48$, $a_2 = 0.40$ and the corresponding rate constants $k_1 = (4\ s)^{-1}$ and $k_2 = (42\ s)^{-1}$ for curve a; $a_1 = 0.78$, $a_2 = 0.18$, $k_1 = (1\ s)^{-1}$, and $k_2 = (51\ s)^{-1}$ for curve b; the amplitudes a_1 and a_2 are units of $Q_A^{-\bullet}$ formed per 230 Chls.

Figure 2) with rate constants of $k_1 \approx (4.0\ s)^{-1}$ and $k_2 = (42\ s)^{-1}$ and amplitudes of 0.48 and 0.40 Q_A per 230 Chl, respectively; (iii) addition of DCMU does not affect either the extent or the rate of $Q_A^{-\bullet}$ accumulation in dry films; and (iv) as compared with untreated material, light-induced $Q_A^{-\bullet}$ formation is much faster in high pH-treated samples that are lacking a functional WOC and all Cyt b559 attaining the LP form (curve b). As shown by the curve b, a 10 s illumination with saturating CW light produces $Q_A^{-\bullet}$ in about 80% of the PS II centers. Similar fast kinetics of Q_A photoreduction were found (data not shown) also in dry films of PS II membranes where the Mn cluster has been deprived by a hydroxylamine treatment that leaves the HP form of Cyt b559 largely uneffected (see Materials and Methods). These findings show that in samples without a functionally competent WOC extent and rate of $Q_A^{-\bullet}$ photoaccumulation are virtually independent of the presence of HP Cyt b559.

The results presented in Figure 2 are very important for understanding the mechanism of electron transfer reactions in dehydrated samples of PS II. They show that the charge separation between P680 and Q_A is not seriously affected in dry films. Therefore, a slower photoaccumulation of dark stable $Q_A^{-\bullet}$ in dry films of PS II membrane fragments containing the WOC has to be explained by other effects. The virtually DCMU insensitive kinetics of $Q_A^{-\bullet}$ formation suggests that the electron transfer between Q_A and Q_B is largely blocked in dry films of PS II membrane fragments.

Photooxidized Cyt b559 is rather stable in dry samples, i.e., it becomes rereduced in the dark in a time domain of tens of minutes (see Figure 8). To characterize the effect of dehydration in more detail, the time course of the light-induced Cyt b559 redox changes and the dependence on the RH were analyzed. Figure 3 shows the light-induced changes of the Cyt b559 redox state (monitored by the bleaching of 560 nm band) as a function of illumination time in buffer

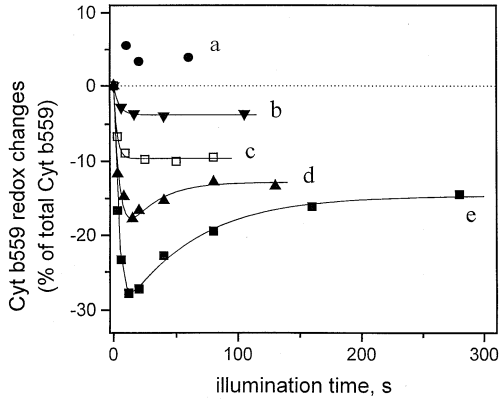

FIGURE 3: Normalized extent of Cyt b559 redox changes as a function of illumination time of untreated PS II membrane fragments either in aqueous buffer suspensions (trace a) or in the form of films of different dehydration levels (traces b−e). In sample a, oxygen-evolving PS II membranes were suspended in standard medium. Films prepared from oxygen-evolving PS II membrane fragments were dehydrated to 89 (b), 65 (c), 43 (d), and 30% RH (e). Difference spectra were monitored in the spectral region between 520 and 590 nm after different times of illumination with red light of PFD of 2200 $\mu Em^{-2}\ s^{-1}$. In ordinate, the negative sign of Cyt b559 redox changes is for photooxidation and the positive sign is for photoreduction.

suspension (trace a) and in dehydrated films of different RH (traces b−e) prepared with oxygen-evolving PS II membrane fragments. The results obtained exhibit three striking features: (i) in all dehydrated samples, the illumination causes a net Cyt b559 oxidation while in suspension of PS II membrane fragments a small but reproducible Cyt b559 photoreduction was detected; (ii) the extent of the initial Cyt b559 oxidation in dehydrated films increases with progressing drying degree; and (iii) below a dehydration threshold, the initial photooxidation is followed by a slower photoreduction of Cyt b559 (traces d and e). Further drying of films to RH levels below 30% virtually did not change the typical curve represented by trace e (vide infra).

When considering the photoinduced oxidation and reduction of Cyt b559 as independent reactions, the pattern can be described by the equation

$$\Delta\text{Cyt b559}(t) = a_{ox}(e^{-k_{ox}t} - 1) + a_{red}(1 - e^{-k_{red}t}) \quad (1)$$

where negative values of ΔCyt b559 reflect a net increase of oxidized Cyt b559 as compared with the dark overall redox state.

Fitting of the data presented by curve e of Figure 3 results in the following values: a_{ox} and $a_{red} = 32$ and 18% of total Cyt b559, respectively, and k_{ox} and $k_{red} = 3.9$ and $(59\ s)^{-1}$, respectively. The amplitudes and rates of Cyt b559 photooxidation and photoreduction are in correspondence with the fast and slow phase, respectively, of $Q_A^{-\bullet}$ formation in this sample type (see curve a in Figure 2).

The reactions induced by CW light are multiturnover processes that are much slower than the elementary electron transfer steps in PS II. It is therefore worth analyzing the time course of the Cyt b559 reactions at different PFDs of actinic light. Figure 4 summarizes the results obtained at two PFDs in a film prepared with oxygen-evolving PS II membrane fragments and dehydrated to 6−8% RH. Curve a was obtained with the same PFD as used for the data

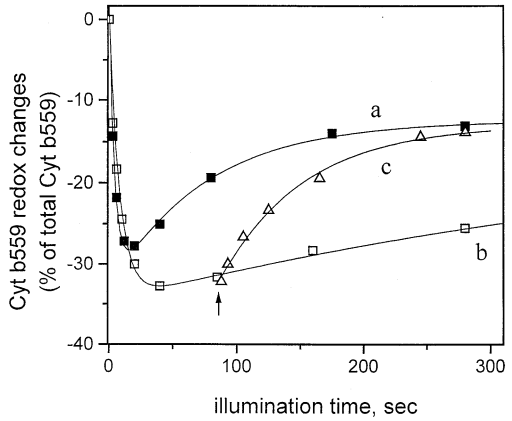

FIGURE 4: Normalized extent of Cyt b559 redox change as a function of illumination time in dry films of untreated PS II membrane fragments. Samples of oxygen-evolving PS II membranes were dehydrated to 6−8% RH. Illumination was performed with red light of 2200 (trace a) and 440 μEm^{-2} s^{-1} (trace b). Sample c was illuminated for 80 s at 440 μEm^{-2} s^{-1}, followed by illumination at 2200 μEm^{-2} s^{-1} (the switching of light is indicated by an arrow). Curve fitting of the experimental data was based on the function $\Delta Cyt\ b559(ox) = a_{ox}(e^{-k_{ox}t} - 1) + a_{red}(1 - e^{-k_{red}t})$ where a_{ox} and a_{red} are the extrapolated maximum extent of Cyt b559 photooxidation and photoreduction, respectively, and k_{ox} and k_{red} are the corresponding rate constants. All amplitudes are presented as % of total Cyt b559. Values were used as follows: a_{ox} = 33%, a_{red} = 21%, k_{ox} = $(4.5\ s)^{-1}$, and k_{red} = $(73\ s)^{-1}$ for curve a; a_{ox} = 35%, a_{red} = 21%, k_{ox} = $(8.5\ s)^{-1}$, and k_{red} = $(480\ s)^{-1}$ for curve b; a_{red} = 21% and k_{red} = $(75\ s)^{-1}$ for curve c.

depicted in Figures 1−3, i.e., 2200 μEm^{-2} s^{-1}. It closely resembles curve e in Figure 3 for a sample dehydrated to 30% RH. A decrease of PFD by a factor of 5, i.e., to 440 μEm^{-2} s^{-1}, affects the kinetics of Cyt b559 photooxidation only by a factor of about 2 but highly retards the rate of the subsequent photoreduction (curve b). As a consequence of these kinetic effects, the apparent maximum extent of Cyt b559 photooxidation is larger in the case of low PFD illumination. To illustrate the effect of actinic illumination on Cyt b559 photoreduction, the sample was illuminated at 440 μEm^{-2} s^{-1} for 80 s, followed by actinic light at 2200 μEm^{-2} s^{-1} (curve c). In case of sufficiently weak light, Cyt b559 photooxidation appears to attain its maximal amplitude and the extent of subsequent reduction remained small. The increase of PFD by a factor of 5 resulted in the onset of a pronounced Cyt b559 photoreduction (curve c) with kinetics and extent similar to that observed when only high PFD light was used (curve a). The resolved heme photoreduction (curve c) is characterized by a k_{red} of $(75\ s)^{-1}$ and an amplitude a_{red} of 21% of Cyt b559.

Figure 5 shows the rate constant for Cyt b559 photoreduction in dry films of untreated PS II membrane fragments as a function of PFD of actinic light. The data reveal a striking dependence of k_{red} on PFD with a characteristic sigmoidal shape. Below a threshold of 400−600 μEm^{-2} s^{-1}, which nearly saturates the Cyt b559 photooxidation, the rate of Cyt b559 photoreduction is negligibly small whereas the maximum value of k_{red} (about $(50\ s)^{-1}$) is reached in a rather narrow range of PFD values.

An interesting phenomenon concerning the Cyt b559 photoreactions in dry films of oxygen-evolving PS II membranes is the lower extent of heme photoreduction as compared to the amplitude of its initial photooxidation. This

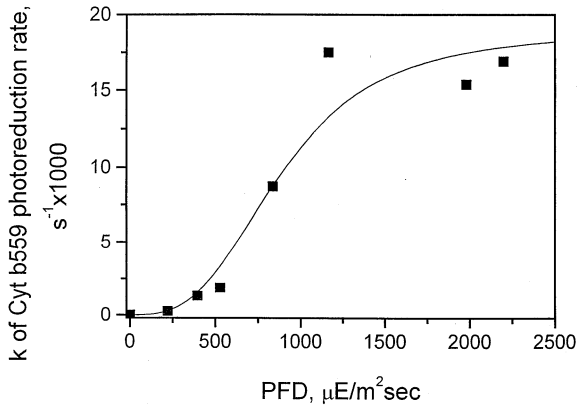

FIGURE 5: Rate constant of the slow phase of Cyt b559 photoreduction as a function of PFD of actinic illumination. Experiments analogues to one shown in curve c of Figure 4 were performed on films of untreated PS II membranes dehydrated to 8−12% RH at different PFD of actinic light.

leads to a net Cyt b559 oxidation after prolonged illumination (Figure 3, curve e, and Figure 4, curves a,c). To check for an effect of molecular oxygen as a possible oxidant of reduced Cyt b559, a dry sample was prepared and the subsequent measurements were performed under anaerobic conditions (i.e., drying was performed under a flow of nitrogen and the cell was then, as usually, hermetically sealed). The results obtained were virtually the same as in the aerobic sample with respect to both amplitude and kinetics of Cyt b559 photoreduction (data not shown).

The increasing extent of Cyt b559 photooxidation with decreasing RH values of the sample is assumed to be related to an impairment of secondary reactions in PS II, namely, the WOC and Q_B function. It is therefore important to study the light-induced reactions in samples that are deprived of a functionally competent WOC. In the following experiments, heme b559 photooxidation was compared in normal and hydroxylamine-treated PS II membrane samples both containing nearly the same fraction of Cyt b559 in its HP redox form (see Materials and Methods). For the sake of direct comparability of the results, the treatment was performed very carefully in order to avoid a significant transformation of HP Cyt b559.

In Figure 6A, the time course is shown of Cyt b559 photooxidation induced by actinic light of PFD = 440 μEm^{-2} s^{-1} in normal and hydroxylamine-treated PS II membrane fragments (traces a and b, respectively). Panel B summarizes the results of subsequent Cyt b559 photoreduction under strong illumination with PFD = 2200 μEm^{-2} s^{-1}. For comparison, traces c and d reflect the corresponding reaction pattern of buffer suspensions of both types of PS II membrane fragments.

An inspection of the data in panel A of Figure 6 leads to two relevant conclusions: (i) the maximum extent of Cyt b559 photooxidation in dry films of PS II membrane fragments is virtually independent of the presence of an intact WOC while the rate is faster by a factor of about two in samples deprived of the WOC (compare traces a and b), and (ii) in suspensions, a photoaccumulation of oxidized Cyt b559 can be only observed in hydroxylamine-treated PS II membrane fragments but not at all in the untreated control where even a slight photoreduction takes place (compare traces c and d). Furthermore, the extent of Cyt b559

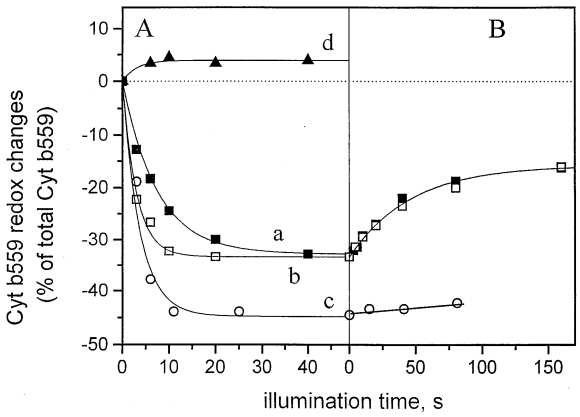

FIGURE 6: Normalized extent of Cyt b559 redox change as a function of illumination time in untreated and hydroxylamine-treated PS II membrane fragments. Films of untreated (filled squares) and hydroxylamine-treated (open squares) PS II membranes were dehydrated to 9 and 12% RH, respectively. For a comparison, the data of the samples are shown in buffer suspension (standard medium) of untreated (filled triangles) and hydroxylamine-treated (open circles) PS II membrane fragments. Actinic light: 440 (panel A) and 2200 μEm^{-2} s^{-1} (panel B). The solid curves of panels A and B are exponentials of the type ΔCyt b559(ox) = $a_{ox}(e^{-k_{ox}t} - 1)$ and ΔCyt b559(red) = $a_{red}(1 - e^{-k_{red}t})$, respectively, with a_{ox} = 33%, k_{ox} = (7.5 s)$^{-1}$ (curve a); a_{ox} = 33%, k_{ox} = (3.0 s)$^{-1}$ (curve b); a_{ox} = 45%, k_{ox} = (3.7 s)$^{-1}$ (curve c); and a_{red} = 18%, k_{red} = (45 s)$^{-1}$ (panel B). All amplitudes are presented as % of total Cyt b559.

photooxidation in dry films of hydroxylamine-treated samples is limited at 33% of the total Cyt b559 while in a buffer suspension of this material almost all initially reduced in the dark Cyt b559 undergoes photooxidation, i.e., levels of 45−50% of total Cyt b559 are reached. In contrast to the phenomena observed for Cyt b559 photooxidation, the kinetics of photoreduction under strong actinic light is independent of the WOC intactness in dry films while no Cyt b559 photoreduction was detected in a buffer suspension of hydroxylamine-treated sample (see panel B).

The results reported in Figure 3 have shown that the pattern of light-induced Cyt b559 photoreactions depends on the hydration degree of the sample. To illustrate this effect in more detail, comparative measurements were performed in films of normal and hydroxylamine-treated PS II membrane fragments dehydrated to different RH levels. For a better separation of oxidation and reduction processes, the samples were at first illuminated with actinic light of 440 μEm^{-2} s^{-1} to resolve the former reaction, followed by exposure to stronger light (2200 μEm^{-2} s^{-1}) for monitoring the latter process as outlined above (for an example, see trace c in Figure 4). The results gathered from these experiments are presented in Figure 7A (for Cyt b559 photooxidation) and B (for Cyt b559 photoreduction).

The traces in panel A of Figure 7 reveal that films of untreated (curve a) and hydroxylamine-treated (curve b) PS II membrane fragments are characterized by an opposite dependence on RH of the extent of Cyt b559 photooxidation. Surprisingly, in dry films, both sample types exhibit the same degree of Cyt b559 photooxidation at an amount of 33% of total Cyt b559, i.e., only about 60% of the initially reduced Cyt participates in the reaction. With increasing RH, the amplitudes of Cyt b559 photooxidation in both samples approach those of the corresponding buffer suspensions (open symbols) that are put formally at 100% RH, i.e., photooxidation of almost 50% of Cyt b559 in hydroxylamine-treated and slight photoreduction in untreated samples. The amplitudes of heme b559 photoreduction decrease in both sample types with progressing film hydration (panel B). The variation of the extent of Cyt b559 photooxidation covers a comparatively wide range of RH (from 30 to 90%) while the dependence of heme photoreduction is restricted to a significantly narrower RH region (30−70%).

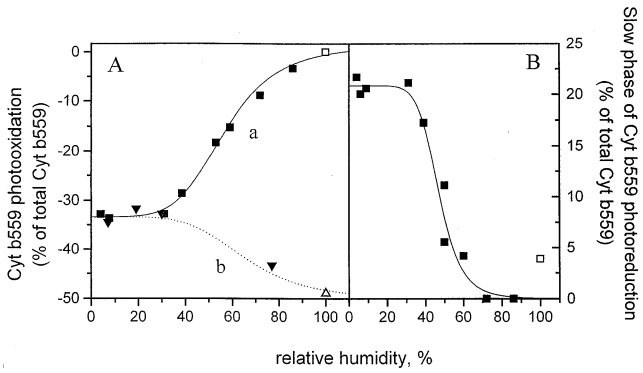

FIGURE 7: Normalized extent of Cyt b559 photooxidation (panel A) and photoreduction (panel B) as a function of RH in films of untreated and hydroxylamine-treated PS II membrane fragments. Data obtained for dehydrated films of untreated and hydroxylamine-treated PS II membranes are symbolized by filled squares and inverted triangles, respectively. Open symbols represent the results for suspensions of the correspondent preparations in standard medium. Actinic illumination with red light: 440 μEm^{-2} s^{-1} for photooxidation and 2200 μEm^{-2} s^{-1} for photoreduction; in the latter case, samples were preilluminated for 80 s with 440 μEm^{-2} s^{-1} to achieve maximum extent of Cyt b559 photooxidation.

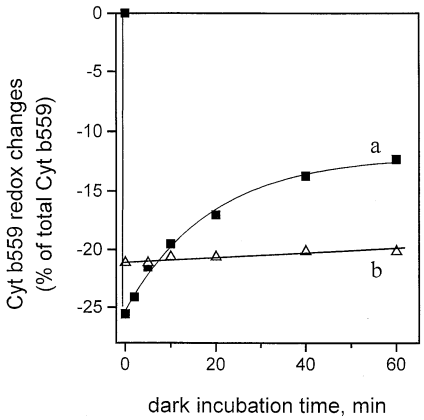

FIGURE 8: Dark recovery of photooxidized Cyt b559 in dry films of untreated PS II membrane fragments. Films of samples in the absence (filled squares) or presence (open triangles) of 50 μM DCMU were dehydrated to 8% RH. Cyt b559 photooxidation was induced by 10 s of illumination with red light of 2200 μEm^{-2} s^{-1}.

Figure 8 shows results obtained for the stability in the dark of Cyt b559 oxidized by short illumination with strong light in dry films of untreated PS II membrane fragments in the absence (a) or presence (b) of DCMU. Very similar time-dependent curves were obtained in dry films of hydroxylamine-treated preparation (data not shown). Trace a in Figure 8 reveals that photooxidized Cyt b559 becomes slowly rereduced reaching a half level after 60 min of dark incubation. The dark reduction is inhibited by DCMU as illustrated by trace b.

The results presented so far show that in dry films (≤30% RH), the pattern of Cyt b559 redox reactions induced by actinic red light is characterized by a fast photooxidation

followed by a much slower partial photoreduction. Except for the rate of photooxidation, this pattern is almost independent of the presence of an intact WOC. In the following, experiments were performed with samples where virtually all Cyt b559 was oxidized in the dark. This enabled us to study exclusively the heme b559 photoreduction.

Two different approaches have been used for dark oxidation of Cyt b559 in preparations of PS II membrane fragments. The first method is a chemical oxidation of the HP form by $K_3[Fe(CN)_6]$ and subsequent washing of the sample to remove the oxidant (see Materials and Methods). The second approach is a pH-induced conversion of the HP form into the LP form followed by its autoxidation. In our previous studies, we showed that incubation at temperatures below 15 °C of oxygen-evolving PS II membrane fragments in high pH (about 9) buffer containing $K_3[Fe(CN)_6]$ resulted in transformation of the HP Cyt b559 into the IP form (51). This IP form is unstable at pH 9 at elevated temperatures and easily converted into the LP form. Accordingly, oxygen-evolving PS II membrane fragments were incubated at pH 9.2 in the presence of 0.5 mM $K_3[Fe(CN)_6]$ at 25 °C (for further details, see Materials and Methods) and subsequently washed to remove the oxidant from the suspension that is shifted back to pH 6.5. The high pH treatment leads to a concomitant loss of the oxygen evolution capacity and homogeneous population of a single LP redox form of Cyt b559 with a E_m of 77 ± 18 mV at pH 6.5 (average of three titrations, data not shown).

Typical results obtained with these two types of preparations are presented in Figure 9. It shows the light-induced difference spectra after three illumination times in dry films of $K_3[Fe(CN)_6]$-washed (panel A) and high pH-treated (panel B) PS II membrane fragments. The spectra are normalized to the same optical density of the samples. The traces indicate that in both samples the actinic light induces photoreduction of both Q_A (detected as C550 signal) and Cyt b559 characterized by the increase in its α-peak at 560 nm. An increasing bleaching at wavelengths below 530 nm due to progressing illumination time is ascribed to accompanying Car oxidation (a more detailed illustration of this effect is shown in Figure 11). An inspection of the difference spectra in panels A and B reveals that the amplitudes of photoreduced Cyt b559 at the same time intervals are virtually the same in both sample types. However, some differences are seen in the time course of $Q_A^{-\bullet}$ photoaccumulation. This reaction appears to be slower in ferricyanide-washed WOC-containing samples than in high pH-treated PS II preparation.

The kinetics of Cyt b559 photoreduction in dry films of PS II membrane fragments were gathered from a quantitative evaluation of difference spectra monitored after different times of actinic illumination. These data are summarized in Figure 10. Curves a and b were obtained for PS II membrane fragments either preoxidized with $K_3[Fe(CN)_6]$ or treated at high pH PS II membranes and actinic illumination of PFD of 2200 $\mu Em^{-2}\ s^{-1}$, while in curve c high pH-treated samples were illuminated at 10-fold lower PFD of 220 $\mu Em^{-2}\ s^{-1}$. DCMU was added to the samples to demonstrate that it does not block Cyt b559 photoreduction. The only insignificant effect of DCMU was in a decrease of the amplitude of a small (~5%) very slow phase of heme b559 photoreduction (in hundreds of s scale) at the expense of faster components.

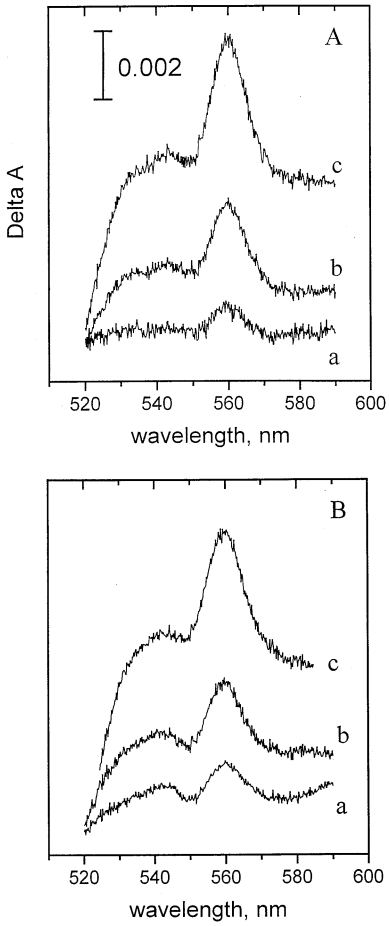

FIGURE 9: Light-induced difference spectra in dry samples of PS II membranes with initially oxidized Cyt by pretreatment with either $K_3[Fe(CN)_6]$ (panel A) or high pH (panel B). Films of ferricyanide-washed (A) and high pH-treated (B) PS II membrane fragments were dehydrated to 7% RH and illuminated by red light of 2200 $\mu Em^{-2}\ s^{-1}$. For further experimental details, see the text and the Materials and Methods. Optical density at 623 minus 750 nm in both samples was 0.82 A. Difference spectra were taken after 6 (a), 40 (b), 400 (trace c in panel A), and 520 s (trace c in panel B) of illumination. The ordinate axis scale in panel B is the same as in panel A.

A numerical analysis of the data reveals that the time course of Cyt b559 photoreduction can be satisfactorily described by biphasic kinetics in both sample types:

$$\Delta Cyt_{red}(t) = a_1(1 - e^{-k_1 t}) + a_2(1 - e^{-k_2 t}) \qquad (2)$$

The fit of curve a leads to amplitude factors a_1 and a_2 of 19 and 23% of total Cyt b559, respectively, and rate constants $k_1 = (8.1\ s)^{-1}$ and $k_2 = (57\ s)^{-1}$. For curve b, corresponding values of 9 and 24%, respectively, are obtained for amplitudes a_1 and a_2 and $k_1 = (8.0\ s)^{-1}$ and $k_2 = (60\ s)^{-1}$ for the rate constants. For the curve c, the amplitudes and rate constants are $a_1 = 9\%$, $a_2 = 24\%$ and $k_1 = (9.0\ s)^{-1}$, $k_2 = (744\ s)^{-1}$, respectively.

A closer inspection of these data shows that the two sample types exhibit similar kinetics at high PFD actinic light with a main difference in the amplitude of the fast component, which is diminished by a factor of about two in the case of high pH-treated preparation. The slower kinetic components in curves a and b closely resemble those observed for Cyt b559 photoreduction in dry films of untreated PS II membrane fragments (see Figures 4 and 6).

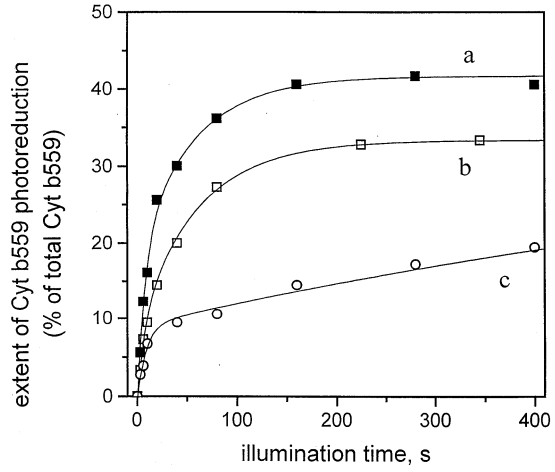

FIGURE 10: Extent of photoreduction of Cyt b559 as a function of illumination time of dry films prepared from $K_3[Fe(CN)_6]$ (closed symbols) and high pH-pretreated PS II membranes (open symbols) in the presence of DCMU. Samples of PS II membrane fragments with preoxidized Cyt b559 containing 40 μM DCMU were dehydrated to 8% RH. Actinic red light: 2200 (squares) and 220 $\mu Em^{-2}\ s^{-1}$ (circles). Full lined curves are biexponential time courses with $a_1 = 19\%$, $a_2 = 23\%$ and $k_1 = (8.1\ s)^{-1}$, $k_2 = (57\ s)^{-1}$ for curve a; $a_1 = 9\%$, $a_2 = 24\%$ and $k_1 = (8\ s)^{-1}$, $k_2 = (60\ s)^{-1}$ for curve b; $a_1 = 9\%$, $a_2 = 24\%$ and $k_1 = (9\ s)^{-1}$, $k_2 = (744\ s)^{-1}$ for curve c. Amplitudes are presented as % of total Cyt b559.

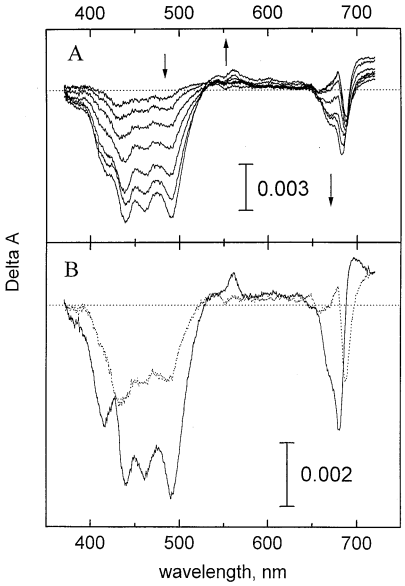

FIGURE 11: Difference spectra obtained upon illumination of dry film of high pH-treated PS II membranes in the presence of DCMU as a function of illumination time. A PS II sample containing 40 μM DCMU was dehydrated to 7% RH under a flow of dry nitrogen. Light-induced difference spectra were monitored after different times of actinic illumination. The arrows indicate increasing time. The first three difference spectra show the data obtained after 3, 6, and 20 s of illumination with red light of PFD = 440 $\mu Em^{-2}\ s^{-1}$; the following four spectra were monitored after additional illumination with red light of PFD = 2200 $\mu Em^{-2}\ s^{-1}$ for 20, 60, 120, and 180 s (panel A). In panel B, spectra of panel A are shown monitored after 20 s of actinic illumination of 440 $\mu Em^{-2}\ s^{-1}$ (dotted line) and difference between the bottom spectrum of panel A and the dotted lined spectrum (full line). The optical density at 623 minus 750 nm was 0.16 A.

A very interesting feature was found for the dependence of Cyt b559 photoreduction on the PFD of actinic illumination. The comparison of curves b and c reveals that the rate of the slow phase of Cyt b559 photoreduction largely decreases at low PFD in accordance with the data described above for the sample of untreated PS II membrane fragments (Figures 4 and 5). In marked contrast, amplitude and rate of the fast kinetics are virtually unaffected when PFD is diminished by a factor of 10.

It has to be emphasized that in most of the experiments reported in the present paper no special efforts were undertaken to remove the oxygen from the sample cell because check experiments under strict anaerobic conditions did not reveal any detectable difference. On the other hand, it is well-known that stable photoreduction of LP Cyt b559 is possible to observe only under anaerobic conditions (*55*, *57*, *80*) as this redox form is autooxidizable. Therefore, the finding of stable LP Cyt b559 photoreduction indicates that anaerobic conditions were created in dry samples, probably due to a prevention of oxygen diffusion inside a dehydrated film.

To obtain more information on redox components that are involved in the light-induced reduction of Cyt b559, difference spectra were monitored in the whole visible range after different illumination times. The experiments were performed under anaerobic conditions to exclude interference of reactions with oxygen in order to permit quantitative estimations. Figure 11 depicts the spectra measured in a typical experiment of Cyt b559 photoreduction in the dry film of PS II membrane fragments that were pretreated at high pH. Essentially, the same spectra were obtained when using $K_3[Fe(CN)_6]$-washed samples (data not shown). Panel A of Figure 11 shows the traces recorded with progressing illumination time at two different PFD values of actinic light. To reveal individual spectral features associated with the reactions of Q_A and Cyt b559 photoreduction, the first three spectra were obtained by using an actinic light of diminished PFD (440 $\mu Em^{-2}\ s^{-1}$), which enables $Q_A^{-\bullet}$ formation in a significant portion of PS II centers accompanied by only minor Cyt b559 photoreduction. A subsequent increase of the actinic light to a PFD value of 2200 $\mu Em^{-2}\ s^{-1}$ gives rise to a large extent of the latter reaction (following four curves). For a better illustration, the dotted line spectrum in panel B reproduces the third spectrum of panel A associated with $Q_A^{-\bullet}$ accumulation and the full line spectrum shows the difference between spectra number 7 (bottom spectrum) and number 3 of panel A reflecting spectral changes that are indicative of Cyt b559 photoreduction.

An inspection of the two curves in panel B reveals marked differences. At a wavelength shorter than 600 nm, the dotted line spectrum is characterized by features due to the formation of C550 whereas the full line spectrum exhibits positive (428, 560 nm) and negative (415 nm) bands in the Soret and α-region of Cyt b559. Both spectra are also characterized by bleaching bands of Chl at 434 nm and Car at 461 and 491 nm indicating that a mixture of oxidized species is formed as a result of illumination. In the red region, more complex spectral changes are observed. The full line spectrum reflects bleaching of Chl whereas the dotted line spectrum in addition exhibits typical features of an electrochromic shift with a negative band at 687 nm and a positive band at 678 nm, which almost exactly corresponds to the electrochromic signal due to $Q_A^{-\bullet}$ formation (*75*, *76*).

The difference spectra shown in Figure 11 indicate that in both photoreactions, i.e., formation of $Q_A^{-\bullet}$ and reduced Cyt b559, the oxidation of both Chl and Car molecules is observed. A mixture of oxidized redox cofactors formed indicates that there is no a preferential electron donor for both photoreduction processes. Rough estimations of the extent of donors oxidation were performed for the spectra presented in panel B by using extinction coefficients of 46 mM^{-1} cm^{-1} at 438 nm (*81*, *82*) and 130 mM^{-1} cm^{-1} at 490 nm (*83*) for Chl and Car cations, respectively. The data evaluation indicates the formation of 0.7 $Chl^{+\bullet}$ and 0.4 $Car^{+\bullet}$ coupled with $Q_A^{-\bullet}$ formation (dotted curve) and 0.9 $Chl^{+\bullet}$ and 1 $Car^{+\bullet}$ accompanying the process of Cyt b559 photoreduction (full lined curve).

DISCUSSION

This paper presents the first detailed study on the reaction pattern in dehydrated samples of PS II membrane fragments. The results obtained reveal that diminished water content in the sample gives rise to three characteristic features with different effects: (i) light-induced formation of the radical pair $P680^{+\bullet}Q_A^{-\bullet}$ is virtually invariant to dehydration down to the lowest values of RH (6−8% RH), as reflected by the extent of photoaccumulation of close to one $Q_A^{-\bullet}$ per 230 Chls; (ii) the electron transfer from $Q_A^{-\bullet}$ to Q_B is severely blocked upon dehydration as deduced from the lack of a DCMU effect on the rate of $Q_A^{-\bullet}$ photoaccumulation; and (iii) the reaction pathway on the PS II donor side becomes drastically modified thus giving rise to a pronounced redox turnover of Cyt b559 at decreasing water content. This effect markedly depends on the integrity of the WOC and levels off below a distinct threshold of RH (at about 30%).

Most of these features closely resemble the reaction pattern of PS II at cryogenic temperatures where the formation of $P680^{+\bullet}Q_A^{-\bullet}$ remains unaffected (*13*, *14*) while both the reoxidation of $Q_A^{-\bullet}$ by Q_B (*15*, *16*, *23*) and $P680^{+\bullet}$ reduction by the WOC (*18*−*20*) are thermally completely blocked and replaced by redox reactions of other components, in particular Cyt b559 (*48*, *79*, *84*−*89*). The general conclusion from the findings of this study is a clear demonstration of the role of water molecules in PS II activity associated with Q_B reduction and the WOC oxidation. It has to be emphasized that the solvating effect comprises a large number of water molecules as clearly seen by the onset of the effects at relatively high RH values and a plateau below a threshold of about 30% RH (see Figure 7). Comparable phenomena have been observed for the electron transport in purple bacteria (*30*−*32*) and for the enzymatic activity of other proteins at low water activity (*24*, *26*, *90*−*92*). The threshold typically observed in similar curves at about 30% RH corresponds with a saturation of polar binding sites in the first layer of water around the protein. It is interesting to note that at this degree of sample hydration a bound spin probe still retains its maximal motional capability while the protein exhibits only a low residual level of functional activity (*24*, *26*, *90*). This phenomenon implies that the water molecules of the higher hydration layers are also important. Repolarization in the total hydration shell or the so-called "biological water" (*93*, *94*) ensures medium reorganization in redox reactions of the Q_B and the WOC. By using quasielastic neutron scattering, it was recently shown for β-lactoglobulin that hydration water affects the dynamics of the whole biomolecule and not only the solvent exposed region (*95*).

The conclusion on the blockage of the WOC in dehydrated samples of PS II membrane fragments is in perfect agreement with a recent FTIR study (*38*). This effect is assumed to comprise both the impairment of $P680^{+\bullet}$ reduction by Y_Z as well as of the redox transitions in the WOC under conditions of restricted medium rearrangement. The adverse effect of freezing on the former reaction has been recently illustrated for samples deprived of the WOC. This reaction becomes progressively retarded below 220 K concomitant with oxidative formation of other radicals ($Chl^{+\bullet}$,$Car^{+\bullet}$) (*96*). An analogous effect is likely to occur in dehydrated samples at room temperature. In samples with a competent WOC, the reduction of $P680^{+\bullet}$ by Y_Z comprises at least three types of rate limitations (*97*) including "large scale" proton shifts (*98*−*100*). It is therefore conceivable that this reaction also becomes impaired in dried PS II membranes with WOC. The details of this phenomenon remain to be clarified.

As a consequence of the impaired WOC function in dehydrated PS II membrane fragments, other electron donors (Cyt b559, Chl, Car) are oxidized by $P680^{+\bullet}$. The present work describes for the first time a detailed quantitative analysis of extent and kinetics of the Cyt b559 redox transitions in dry films of PS II membrane fragments. This analysis enables us to reveal important peculiarities of electron transfer reactions involving Cyt b559.

A very interesting feature emerges from the maximum extent of Cyt b559 photooxidation reached by illumination of dry films of untreated and hydroxylamine-washed PS II membrane fragments. This value levels off at about 33% of the total Cyt b559 although both sample types contain at least 50% in the HP form (see Materials and Methods) that are reduced at the beginning of the experiment. As expected for samples deprived of the WOC function, in the hydroxylamine-treated PS II membrane fragments suspended in buffer, almost all HP Cyt b559 becomes photooxidized (see Figures 6 and 7). A limitation to only about 60% detected photooxidation of the initially reduced HP Cyt b559 cannot be ascribed to residual competing WOC activity in the dry sample because the same level is obtained in films of untreated and hydroxylamine-washed PS II membrane fragments. It is also important to note that the limitations of detected Cyt b559 photooxidation distinctly differs in its origin from the known phenomenon of diminution of the extent of photooxidation of bound Cyt c in purple bacteria upon sample freezing or dehydration (*32*, *101*). In the latter case, the gap between the reduction potentials of the primary donor P and the proximal heme c, respectively, is relatively small, i.e., within the range of 100−120 mV. Accordingly, a restriction of conformational relaxations of the environment due to freezing or dehydration gives rise to formation of nonequilibrium redox states [Cyt c^+/P]* and [Cyt c/P^+]* that are nearly isopotential thus resulting in a significant decrease of the efficiency of the redox reaction (*101*). An analogous effect should be irrelevant for the energetics of Cyt b559 photooxidation because the gap between the reduction potentials of HP Cyt b559 and its redox partner(s) (P680, Car, or Chl) is expected to be very large ($\geq$500 mV).

A straightforward explanation for the restriction of detected Cyt b559 photooxidation in the dry films of PS II membrane

fragments emerges from an inspection of the data presented in Figures 3 and 10. It suggests that in dehydrated samples Cyt b559 is simultaneously photooxidized and photoreduced. As a consequence, the extent of 33% of detected Cyt b559 photooxidation can be interpreted as the result of an overlap of photooxidation comprising 55% of total Cyt b559 and counterbalancing fast photoreduction of about 20% of total Cyt b559. A subsequent slower phase of Cyt b559 photoreduction takes place in a time domain of tens of seconds. Only few papers are known on a parallelism of opposite Cyt b559 photoreactions for samples suspended in buffer solutions (*102*−*105*). This phenomenon was supposed to originate from the involvement of two different Cyt b559 hemes in opposite redox transitions (*102*, *104*). More often, however, assay conditions were selected where only one type of the reactions (either oxidation or reduction of Cyt b559) was observed (*52*, *53*, *56*, *106*−*108*).

The results of our investigations on Cyt b559 photoreduction by endogenous donors in dehydrated films of PS II membrane fragments revealed that this process exhibits the following characteristic features: (i) it is insensitive to DCMU; (ii) the extent of Cyt b559 photoreduction does never exceed 50% of total Cyt b559; (iii) the transformation of oxidized Cyt b559 heme from its HP into the LP form does significantly affect neither the kinetics nor the total extent of Cyt b559 photoreduction; (iv) the process exhibits clearly biphasic kinetics with entirely different sensitivity of the rates of the two components on the intensity of CW illumination; and (v) endogenous components (Chl, Car) act as electron donors for photoreduction of Cyt b559.

The insensitivity to DCMU of Cyt b559 photoreduction in dry films of PS II membrane fragments indicates that Q_B is not involved and that $Q_A^{-\bullet}$ and/or $Pheo^{-\bullet}$ are the electron donors for oxidized Cyt b559. Lack of sensitivity or only weak DCMU dependence have been previously reported for Cyt b559 photoreduction in aqueous buffer suspensions (*55*−*57*, *59*, *71*, *107*, *109*).

Another peculiarity of Cyt b559 photoreduction is the biphasic kinetics in the dehydrated films. A similar kinetic feature of analogous reactions taking place in different time scales has been previously reported for samples in suspension (see, for instance, refs *71*, *80*, *102*, *104*), and both components were found to be DCMU insensitive (*80*, *102*). Because the biphasic kinetic pattern is also observed in dry films, this characteristic has to be ascribed to Cyt b559 photoreduction itself and is not the result of an unsaturated behavior by the soluble redox cofactors used in suspension assays. Furthermore, the two kinetic components significantly differ in their dependence on PFD of actinic illumination where the faster phase corresponds with the time course of $Q_A^{-\bullet}$ formation while the slower phase rather indicates the photoaccumulation of $Pheo^{-\bullet}$. This assignment of the two kinetic components is supported by the sigmoidal dependence on PFD of the rate constant of the slow kinetics of Cyt b559 photoreduction (see Figure 5). This feature indicates that the accumulation of $Q_A^{-\bullet}$ is a necessary prerequisite for the slower process of Cyt b559 photoreduction. Accordingly, a heterogeneity in the pathways of Cyt b559 photoreduction exists; the major fraction of the state Cyt $b559^{ox}Q_A^{-\bullet}$ (80−90%) is stable in the dark, but in a minor fraction (10−20%), Cyt b559 is reduced via a fast electron transfer (in the scale of several seconds) from $Q_A^{-\bullet}$. This reaction is responsible for the diminution of the visible extent of Cyt b559 photooxidation as discussed above. In about 20% of PS II complexes, Cyt b559 is photoreduced by electron transfer from $Pheo^{-\bullet}$ with the maximum rate constant of about $(50\ s)^{-1}$. A comparable value of $(13\ s)^{-1}$ was reported for the rate constant of Cyt b559 photoreduction from $Pheo^{-\bullet}$ in buffer solutions of D1−D2−Cyt b559 complexes in the absence of added quinones (*55*).

Figure 2 shows that similar biphasic kinetics were also found for the rate of photoaccumulation of $Q_A^{-\bullet}$ in dehydrated samples of PS II. This behavior is not related to dehydration itself as the ratio of the amplitudes of the fast and slow phases of photoreduction of Q_A is determined by the sample type. The similarity of the slow kinetics of photoreduction of Cyt b559 and Q_A might suggest that in part of the PS II complexes both reactions are limited in rate due to slow electron transfer from $Pheo^{-\bullet}$.

The key point for the interpretation of the results on the Cyt b559 photoreactions is—in our opinion not fully resolved—the problem of the number of Cyt b559 heme groups in PS II. The recently reported X-ray crystal structure data clearly show that only one Cyt b559 heme group is present in PS II complexes from two different species of thermophilic cyanobacteria (*8*, *9*). These results strongly support the previously claimed dogma of only one Cyt b559 per PS II (for a review, see ref *41* and references therein). However, this dogma is difficult to reconcile with recent data of proteomics analyses that reported the existence of two Cyt b559 per PS II in both mesophilic (*60*) and thermophilic (*61*) cyanobacteria. This puzzling discrepancy could originate in either the use of an incorrect difference extinction coefficient or the existence of a second fragile copy of Cyt b559 in PS II from cyanobacteria that is easily lost during PS II core complex preparation. For PS II of higher plants, the question on the Cyt b559 content cannot be answered at all on the basis of the currently available structural data because the best resolution of 8 Å was achieved for samples that are lacking CP43 (and other polypeptides) and deprived of oxygen evolution capacity (*110*). A resolution limit of 10 Å in *x*,*y*-planes and 23.8 Å for the *z*-direction reported for oxygen-evolving PS II core dimer complexes from spinach (*111*) does not permit unambiguous conclusions. Furthermore, striking differences can exist between cyanobacteria and higher plants. A most illustrative example is the stoichiometry of the manganese-stabilizing extrinsic 33 kDa protein. Cyanobacteria contain only one copy seen in the X-ray crystal structure (*8*, *9*) while two copies were found in higher plants (*112*). An analogous feature cannot be a priori excluded for Cyt b559.

Another interesting aspect on the possible arrangement of a second Cyt b559 in PS II should be taken into consideration, i.e., the rapid turnover of the D1 protein (for a review, see ref *113* and references therein). The repair cycle requires that D1 can be replaced without drastic structural changes of the whole PS II complex. This could imply that a putative second Cyt b559 might be weakly bound and prone to a loss during PS II core preparations. As a result of the abovementioned discussion, one should keep in mind the possibility to question the dogma of one Cyt b559 per PS II for higher plants.

Regardless of the detailed mechanism, electron transfer from $Q_A^{-\bullet}$ and $Pheo_A^{-\bullet}$ to Cyt b559 at a reasonable rate requires that the distance between the donor and the heme group is not too large (*114*−*116*). Accordingly, in former schemes, the Cyt b559 heme had been provisionally placed closer to Q_A than to Q_B (*57*, *59*, *71*). However, on the basis of the recent X-ray crystallographic structure data (*8*, *9*), this order has to be reversed with edge to edge distances from the heme group of Cyt b559 to Q_A and Q_B of the order of 45 and 25 Å, respectively. As a consequence, a direct electron transfer from $Q_A^{-\bullet}$ to the heme group of Cyt b559 cannot take place in a reasonable time when taking into account empirical rate constant−distance relationships (*114*−*116*) based on the Marcus theory for nonadiabatic electron transfer (*117*, *118*). The situation is nearly the same for an electron transfer between the Pheo ($Pheo_A$) in the active branch of charge separation and the heme of Cyt b559 because this distance is about 40 Å. Therefore, the participation of at least one redox mediator group (symbolized by X) is indispensable for electron transer from $Q_A^{-\bullet}$ and $Pheo_A^{-\bullet}$ to Cyt b559 at the position determined by structure analyses (*8*, *9*). The putative component mediating Cyt b559 reduction by photoreduced $Q_A^{-\bullet}$ ($Pheo_A$) could be an extra bound quinone molecule in the PS II reaction center as suggested in ref *80*. An alternative possibility is the participation of the Pheo from the inactive branch of PS II ($Pheo_B$) because its edge to edge distance to Cyt b559 is about 22 Å. At present, however, no convincing experimental evidence exists neither for electron transfer via the inactive branch nor from $Pheo_A$ to $Pheo_B$. A much simplier interpretation is achieved with PS II models containing two Cyt b559 at different positions (vide infra).

A very important finding of the present work is the observation that no more than 50% of the total Cyt b559 heme can be photoreduced by endogenous electron donors (Chl, Car) in dry films of PS II membrane fragments, which are fully photochemically competent (as inferred on the basis of $Q_A^{-\bullet}$ formation). This functional heterogeneity in the Cyt b559 population was observed even in samples that exhibit homogeneous redox properties due to transformation of all Cyt b559 into the LP form by high pH treatment of PS II membrane fragments. One possibility for only partial photoreduction of the whole LP−Cyt b559 population is the existence of a cyclic flow of electrons through Cyt b559 in dry films of PS II membrane fragments with Cyt b559 acting as both electron donor and electron acceptor. It should be emphasized that cyclic electron transfer around PS II including Cyt b559 is a widely accepted hypothesis but this mechanism implies the participation of the Q_B site and of mobile plastoquinone molecule(s) of the pool. This mode of cycle cannot take place in the dry samples because our data show that the electron flow from $Q_A^{-\bullet}$ to Q_B is interrupted upon dehydration. An alternative is a heterogeneity in PS II complexes, either in terms of the existence of an intrinsic additional electron transfer pathway (e.g., related to putative bound intermediate(s) of electron transfer between $Q_A^{-\bullet}$/$Pheo_A^{-\bullet}$ and ferri-Cyt b559) or by creating a new channel (another type of cyclic electron flow) in a fraction of the sample upon dehydration. A check for these possibilities requires further extensive investigations that are far beyond the scope of the present study.

Figure 11 shows that in dry films of PS II membrane fragments containing virtually all Cyt b559 in the oxidized state, $Q_A^{-\bullet}$ photoaccumulation is accompanied by irreversible photooxidation of Car and Chl molecules. This behavior of dehydrated samples resembles that found at cryogenic temperatures (*119*−*122*). However, Cyt b559 photoreduction has not been reported for frozen samples. Here, we show that in dehydrated PS II films Car and Chl are irreversibly oxidized during photoreduction of Cyt b559 and Q_A. Interestingly, it was found earlier that freezing of D1−D2−Cyt b559 complexes under illumination gives rise to a trapped state that does not recombine at 77 K with photoreduced Cyt b559 and an oxidized Chl molecule (*123*). This feature closely resembles the finding of the present paper.

Electron donation from Cyt b559 to $P680^{+\bullet}$ is considered to occur via Car, where the cation radical $Car^{+\bullet}$ oxidizes the heme of b559 either directly (*119*, *120*) or through a redox active Chl (*89*, *121*). At present, it is not yet absolutely clear which side of the PS II reaction center (D1 side or D2 side) is active in auxiliary electron transfer to $P680^{+\bullet}$ (see refs *121* and *124* and references therein). The simultaneous and stable light-induced formation of reduced Cyt b559 and oxidized radicals $Chl^{+\bullet}$ and $Car^{+\bullet}$ in dry films of PS II membrane fragments shown in Figure 11 suggests that these species are separated by a distance sufficiently long to prevent back reactions.

In marked contrast to the DCMU insensitive Cyt b559 photoreduction in the dehydrated films, the very slow partial rereduction of photooxidized Cyt b559 in the dark is blocked by DCMU (see Figure 8). The latter phenomenon indicates that the Q_B site is involved in this reaction. The electron donor for a part of the photooxidized Cyt b559 could be a Q_B^- population that is stable in the dark in a fraction of PS II complexes. In a former study (*67*), a similar DCMU sensitive dark reduction of photooxidized HP Cyt b559 was reported for aqueous thylakoid suspensions. This reaction takes place in a time domain of several minutes thus indicating a slow redox equilibrium between the two species.

The interpretation described so far for the results obtained in this study is based entirely on the dogma of only one Cyt b559 existing in each PS II complex of all oxygen-evolving photosynthetic organisms. It reveals that some serious assumptions on sample heterogeneity and additional electron transfer pathways have to be introduced in order to account for the experimental data. Therefore, keeping in mind the open questions related to this dogma (vide supra), we would like to add at the end of this paper a very brief interpretation within an alternative model of two Cyt b559 per PS II. We will only discuss the possible situation of higher plants. In this case, it is proposed that two Cyt b559 type heme groups are bound in the PS II complex near the stroma side: one in closer proximity to Q_B (Cyt $b559_B$) as known from the structure of thermophilic cyanobacteria (*8*, *9*) and the other one closer to Q_A (Cyt $b559_A$). Furthermore, Cyt $b559_A$ is assumed to be more vulnerable in redox potential than Cyt $b559_B$. Therefore, in typical preparations of PS II membrane fragments from higher plants (spinach), the PS II complexes are characterized by a dominating state Cyt $b559_A$ (LP)/Cyt $b559_B$ (HP) (to simplify the consideration, no explicit distinction is made between the IP and LP forms of Cyt b559). In dry samples with blocked electron transfer from

Q_A to Q_B, only Cyt $b559_A$ can be photoreduced (from $Q_A^{-\bullet}$ and $Pheo^{-\bullet}$) and only Cyt $b559_B$ can be photooxidized. The existence of a redox equilibrium between Q_A and Cyt $b559_A$ would explain the similarity in kinetics of photoreduction of both species. Likewise, the simultaneous light-induced formation of state $(Cyt\ b559_A)_{red}(Car, Chl)_{ox}$ and its high dark stability in dry films of PS II membrane fragments (Figure 11) are easily explainable by the assumption that the electron donors Chl and Car are bound in the D1/D2 heterodimer at sufficiently long distances to $(Cyt\ b559_A)_{red}$.

CONCLUDING REMARKS

The present study has shown that in PS II "biological" water plays a key role for the integrity of the physiological electron transport pathway from water to PQ in the Q_B site. Under physiological conditions, the Cyt b559 reactions are probably of minor relevance because the fast kinetics of water oxidation to molecular oxygen and PQ reduction to PQH_2 dominate the reaction pattern. However, under stress conditions affecting the WOC and the Q_B functions and in newly synthesized PS II complexes that are lacking the WOC, the redox reactions of the heme groups of Cyt b599 exert a significant protective function.

ACKNOWLEDGMENT

We thank Dr. A. Zouni and J. Kern for valuable discussions on the PS II structure and information on distances between cofactors in PS II, Prof. G. Brudvig for stimulating comments, and Dr. K.-D. Irrgang for helpful suggestions in carrying out the experiments.

REFERENCES

1. Renger, G. (1992) in *Topics in Photosynthesis, The Photosystems: Structure, Function and Molecular Biology* (Barber, J., Ed.) pp 45−99, Elsevier, Amsterdam.
2. Diner, B. A., and Babcock, G. T. (1996) in *Advances in Photosynthesis, Oxygenic Photosynthesis: the Light Reactions* (Ort, D. R, Yocum, C. F., Eds.) Vol. 4, pp 213−247, Kluwer, Dordrecht.
3. Crofts, A. R., and Wraight, C. A. (1983) *Biochim. Biophys. Acta 726*, 149−185.
4. Lavergne, J., and Briantais, J.-M. (1996) in *Advances in Photosynthesis, Oxygenic Photosynthesis: the Light Reactions* (Ort, D. R, Yocum, C. F., Eds.) Vol. 4, pp 265−287, Kluwer, Dordrecht.
5. Debus, R. J. (1992) *Biochim. Biophys. Acta 1102*, 269−352.
6. Yachandra, V. K., Sauer, K., and Klein, M. P. (1996) *Chem. Rev. 96*, 2927−2950.
7. Renger, G. (1999) in *Concepts in Photobiology: Photosynthesis and Photomorphogenesis* (Singhal, G. S, Renger, G., Govindjee, Irrgang, K.-D., Sopory, S. K., Eds.) pp 292−329, Kluwer Academic Publishers, Dordrecht, Narosa Publishing Co., Delhi.
8. Zouni, A., Witt, H. T., Kern, J., Fromme, P., Krauss, N., Saenger, W., and Ort, P. (2001) *Nature 409*, 739−743.
9. Kamiya, N., and Shen, J.-R. (2003) *Proc. Natl. Acad. Sci. U.S.A. 100*, 98−103.
10. Frauenfelder, H., Parak, F., and Young, R. D. (1988) *Annu. Rev. Biophys. Chem. 17*, 451−479.
11. Frauenfelder, H., Sligar, S. G., and Wolynes, P. G. (1991) *Science 254*, 1598−1603.
12. Frauenfelder, H., and McMahon, B. G. (1998) *Proc. Natl. Acad. Sci. U.S.A. 95*, 4795−4797.
13. Reinman, S., and Mathis, P. (1981) *Biochim. Biophys. Acta 635*, 249−258.
14. Prokhorenko, V. I., and Holzwarth, A. R. (2000) *J. Phys. Chem. B 104*, 11563−11578.
15. Joliot, A., and Joliot, P. (1964) *C. R. Acad. Sci. Paris 258*, 4622−4625.
16. Eckert, H.-J., and Renger, G. (1988) *FEBS Lett. 236*, 425−431.
17. Reifarth, F., and Renger, G. (1998) *FEBS Lett. 428*, 123−126.
18. Koike, H., and Inoue, Y. (1987) in Progress in Photosynthesis Research (Biggins, J., Ed.) Vol. I, pp 645−648, Martinus Nijhoff, Dordrecht.
19. Styring, S., and Rutherford, A. W. (1988) *Biochim. Biophys. Acta 933*, 378−387.
20. Gleiter, H. M., Haag, E., Inoue, Y., and Renger, G. (1993) *Photosynth. Res. 35*, 41−53.
21. Stowell, M. H. B., McPhilips, T. M., Rees, D. C., Soltis, S. M., Abresch, E., and Feher, G. (1997) *Science 276*, 812−816.
22. Xu, Q., Baciou, L., Sebban, P., and Gunner, M. R. (2002) *Biochemistry 41*, 10021−10025.
23. Garbers, A., Kurreck, J., Reifarth, F., Renger, G., and Parak, F. (1998) *Biochemistry 37*, 11399−11404.
24. Rupley, J. A., Gratton, E., and Careri, G. (1983) *Trends Boichem. Soc. 8*, 18−22.
25. Klibanov, A. M. (1989) *Trends Biochem. Soc. 14*, 141−144.
26. Careri, G., Gratton, E., Yang. P.-H., and Rupley, J. A. (1980) *Nature 284*, 572−573.
27. Zaks, A., and Klibanov, A. M. (1984) *Science 224*, 1249−1251.
28. McMahon, B. H., Müller, J. D., Wraight, C. A., and Nienhaus, G. U. (1998) *Biophys. J. 74*, 2567−2587.
29. Palazzo, G., Mallardi, A., Hochkoeppler, A., Cordone, L., and Venturoli, G. (2002) *Biophys. J. 82*, 558−568.
30. Clayton, R. K. (1978) *Biochim. Biophys. Acta 504*, 255−264.
31. Nikolaev, G. M., Knox, P. P., Kononenko, A. A., Grishanova, N. P., and Rubin, A. B. (1980) *Biochim. Biophys. Acta 590*, 194−201.
32. Chamorovsky, S. K., Kononenko, A. A., Petrov, E. G., Pottosin, I. I., and Rubin, A. B. (1986) *Biochim. Biophys. Acta 848*, 402−410.
33. Berg, A. I., Knox, P. P., Kononenko, A. A., Frolov, E. N., Khrymova, I. N., Rubin, A. B., Likhtenstein, G. I., Goldansky, V. I., Parak, F., Bukl, M., and Mossbauer, R. (1979) *Mol. Biol. 13*, 81−89 (in Russian).
34. Schinkel, J. E., Downer, N. W., and Rupley, J. A. (1985) *Biochemistry 24*, 352−366.
35. Aksenov, S. I., Bozhenko, V. K., Kononenko, A. A., Pottosin, I. I., Rubin, A. B., and Chamorovsky, S. K. (1987) *Biophysics 32*, 46−50 (in Russian).
36. Skotnica, J., Matouskova, M., Naus, J., Lazar, D., and Dvorak, L. (2000) *Photosynth. Res. 65*, 29−40.
37. Canaani, O., and Havaux, M. (1990) *Proc. Natl. Acad. Sci. U.S.A. 87*, 9295−9299.
38. Noguchi, T., and Sugiura, M. (2002) *Biochemistry 41*, 2322−2330.
39. Cramer, W. A., and Whitmarsh, J. (1977) *Annu. Rev. Plant Physiol. 28*, 133−172.
40. Whitmarsh, J., and Pakrasi, H. B. (1996) in *Oxygenic Photosynthesis: The Light Reactions* (Ort, D. R., Yokum, C. F., Eds.) pp 249−264, Kluwer Academic Publishers, Netherlands.
41. Stewart, D. H., and Brudvig, G. W. (1998) *Biochim. Biophys. Acta 1367*, 63−87.
42. Herrmann, R. G., Alt, J., Schiller, B., Widger, W. R., and Cramer, W. A. (1984) *FEBS Lett. 176*, 239−244.
43. Widger, W. R., Cramer, W. A., Hermodson, M., and Herrmann, R. G. (1985) *FEBS Lett. 191*, 186−190.
44. Cramer, W. A., Theg, S. M., and Widger, W. R. (1986) *Photosynth. Res. 10*, 393−403.
45. Babcock, G. T., Widger, W. R., Cramer, W. A., Oertling, W. A., and Metz, J. G. (1985) *Biochemistry 24*, 3638−3645.
46. Pakrasi, H. B., De Ciechi, P., and Whitmarsh, J. (1991) *EMBO J. 10*, 1619−1627.
47. Berthomieu, C., Boussac, A., Mäntele, W., Breton, J., and Nabedryk, E. (1992) *Biochemistry 31*, 11460−11471.
48. Thompson, L. K., Miller, A.-F., Buser, C. A., de Paula, J. C., and Brudvig, G. W. (1989) *Biochemistry 28*, 8048−8056.
49. Iwasaki, I., Tamura, N., and Okayama, S. (1995) *Plant Cell Physiol. 36*, 583−589.
50. McNamara, V. P., and Gounaris, K. (1995) *Biochim. Biophys. Acta 1231*, 289−296.
51. Kaminskaya, O., Kurreck, J., Irrgang, K.-D., Renger, G., and Shuvalov, V. A. (1999) *Biochemistry 38*, 16223−16235.
52. Whitmarsh, J., and Cramer, W. A. (1978) *Biochim. Biophys. Acta 501*, 83−93.
53. Heber, U., Kirk, M. R., and Boardman, N. K. (1979) *Biochim. Biophys. Acta 546*, 292−306.
54. Nedbal, L., Samson, G., and Whitmarsh, J. (1992) *Proc. Natl. Acad. Sci. U.S.A. 89*, 7929−7933.

55. Barber, J., and De Las Rivas, J. (1993) *Proc. Natl. Acad. Sci. U.S.A. 90*, 10942−10946.
56. Ortega, J. M., Hervas, M., De la Rosa, M., and Losada, M. (1995) *Photosynth. Res. 46*, 185−191.
57. Poulson, M., Samson, G., and Whitmarsh, J. (1995) *Biochemistry 34*, 10932−10938.
58. Gadjieva, R., Mamedov, F., Renger, G., and Styring, S. (1998) in *Photosynthesis: Mechanisms and Effects* (Garab, G., Ed.) Vol. II, pp 1101−1104, Kluwer, Dordrecht.
59. Manguson, A., Rova, M., Mamedov, F., Fredriksson, P.-O., and Styring, S. (1999) *Biochim. Biophys. Acta 1411*, 180−191.
60. Kashino, Y., Lauber, W. M., Carroll, J. A., Wang, Q., Whitmarsh, J., Satoh, K., and Pakrasi, H. G. (2002) *Biochemistry 41*, 8004−8012.
61. Kashino, Y., Koike, H., Yoshio, M., Egashira, H., Ikeuchi, M., Pakrasi, H., and Satoh, K. (2002) *Plant Cell Physiol. 43*, 1366−1373.
62. Berthold, D. A., Babcock, G. T., and Yocum, C. F. (1981) *FEBS Lett. 134*, 231−234.
63. Völker, M., Ono, T., Inoue, Y., and Renger, G. (1985) *Biochim. Biophys. Acta 806*, 25−34.
64. Tamura, N., and Cheniae, G. (1987) *Biochim. Biophys. Acta 890*, 179−194.
65. Miller, A.-F., and Brudvig, G. W. (1990) *Biochemistry 29*, 1385−1392.
66. Young, J. F. (1967) *J. Appl. Chem. 17*, 241−245.
67. Buser, C. A., Diner, B. A., and Brudvig, G. W. (1992) *Biochemistry 31*, 11449−11459.
68. Dekker, J. P., van Gorkom, H. J., Brok, M., and Ouwehaund, L. (1984) *Biochim. Biophys. Acta 764*, 301−309.
69. Porra, R. J., Thompson, W. A., and Kriedemann, P. E. (1989) *Biochim. Biophys. Acta 975*, 384−394.
70. Renger, G. (1972) *Biochim. Biophys. Acta 256*, 428−439.
71. Mizusawa, N., Yamashita, T., and Miyao, M. (1999) *Biochim. Biophys. Acta 1410*, 273−286.
72. Lam, E., Baltimore, B., Ortiz, W., Chollar, S., Melis, A., and Malkin, R. (1983) *Biochim. Biophys. Acta 724*, 201−211.
73. Buser, C. A., Diner, B. A., and Brudvig, G. W. (1992) *Biochemistry 31*, 11441−11448.
74. Irrgang, K. D., Lekauskas, A., Franke, P., Reifarth, F., Smolian, H., Karge, M., and Renger, G. (1998) in *Photosynthesis: Mechanisms and Effects* (Garab., G., Ed.) Vol. II, pp 977−980, Kluwer Academic Publishers, Dordrecht, The Netherlands.
75. Van Gorkom, H. J., Tamminga, J. J., and Haveman, J. (1974) *Biochim. Biophys. Acta 347*, 417−438.
76. Klimov, V. V., Klevanik, A. V., Shuvalov, V. A., and Krasnovsky, A. A. (1977) *FEBS Lett. 82*, 183−186.
77. Renger, G. (1979) *Biochim. Biophys. Acta 547*, 103−116.
78. Schatz, G. H., and van Gorkom, H. J. (1985) *Biochim. Biophys. Acta 810*, 283−294.
79. Knaff, D. B., and Arnon, D. I. (1969) *Proc. Natl. Acad. Sci. U.S.A. 63*, 956−962.
80. Kruk, J., and Strzalka, K. (2001) *J. Biol. Chem. 276*, 86−91.
81. Borg, D. C., Fajer, J., Felton. R. H., and Dolphin, D. (1970) *Proc. Natl. Acad. Sci. U.S.A. 67*, 813−820.
82. Davis, M. S., Forman, A., and Fajer, J. (1979) *Proc. Natl. Acad. Sci. U.S.A. 76*, 4170−4174.
83. Britton, G., and Yang, A. J. (1993) in *Carotenoids in Photosynthesis* (Yang, A., and Britton, G., Eds.) pp 409−457, Chapman and Hall, London.
84. Butler, W. L., Visser, J. W. M., and Simons, H. L. (1973) *Biochim. Biophys. Acta 325*, 539−545.
85. Vermeglio, A., and Mathis, P. (1973) *Biochim. Biophys. Acta 292*, 763−771.
86. Malkin, R., and Vänngard, T. (1980) *FEBS Lett. 111*, 228−231.
87. Nugent, J. H. A., and Evans, M. C. W. (1980) *FEBS Lett. 112*, 1−4.
88. de Paula, J. C., Innes, J. B., and Brudvig, G. W. (1985) *Biochemistry 24*, 8114−8120.
89. Thompson, L. K., and Brudvig, G. W. (1988) *Biochemistry 27*, 6653−6658.
90. Yang, P.-H., and Rupley, J. A. (1979) *Biochemistry 18*, 2654−2661.
91. Colombo, M. F., Rau, D. C., and Parsegian, V. A. (1992) *Science 256*, 655−659.
92. Launnas, V., and Petit, B. M. (1994) *Proteins Struct., Funct., Genet. 18*, 148−160.
93. Nandi, N., and Bagchi, B. (1997) *J. Phys. Chem. B 101*, 10954−10961.
94. Peon, J., Pal, S. K., and Zewail, A. H. (2002) *Proc. Natl. Acad. Sci. U.S.A. 99*, 10964−10969.
95. Orecchini, A., Paciaroni, A., Bizzarri, A. R., and Cannistraro, S. (2002) *J. Phys. Chem. B 106*, 7348−7354.
96. Kühne, H., and Brudvig, G. W. (2002) *J. Phys. Chem. B 106*, 8189−8196.
97. Renger, G. (2001) *Biochim. Biophys. Acta 1503*, 210−228.
98. Schilstra, M. J., Rappaport, F., Nugent, J. H. A., Barnett, C. J., and Klug, D. R. (1998) *Biochemistry 37*, 3974−3981.
99. Christen, G., and Renger, G. (1999) *Biochemistry 38*, 2068−2077.
100. Christen, G., Seeliger, A., and Renger, G. (1999) *Biochemistry 38*, 6082−6092.
101. Kaminskaya, O., Konstantinov, A. A., and Shuvalov, V. A. (1990) *Biochim. Biophys. Acta 1016*, 153−164.
102. Velthuys, B. R. (1981) *FEBS Lett. 126*, 272−276.
103. Packham, N. K., and Barber, J. (1984) *Biochem. J. 221*, 513−520.
104. Barabas, K., and Garab, G. (1989) *FEBS Lett. 248*, 62−66.
105. Samson, G., and Fork, D. C. (1992) *Photosynth. Res. 33*, 203−212.
106. Ben-Hayyim, G. (1972) *FEBS Lett. 28*, 145−148.
107. Ben-Hayyim, G. (1974) *Eur. J. Biochem. 41*, 191−196.
108. Böhme, H., and Kunert, K.-J. (1980) *Eur. J. Biochem. 106*, 329−336.
109. Yamagishi, A., and Fork, D. C. (1987) *Arch. Biochem. Biophys. 259*, 124−130.
110. Rhee, K.-H., Morris, E. P., Barber, J., and Kühlbrandt, W. (1998) *Nature 396*, 283−286.
111. Hankamer, B., Morris, E., Nield, J., Garle, C., and Barber, J. (2001) *J. Struct. Biol. 135*, 262−269.
112. Popelkova, H., Im, M. M., and Yocum, C. F. (2002) *Biochemistry 41*, 10038−10045.
113. Zhang, L., and Aro, E.-M. (2002) *FEBS Lett. 512*, 13−18.
114. Moser, C. C., and Dutton, P. C. (1996) in *Protein Electron Transfer* (Bendall, D. S., Ed.) pp 1−21, BIOS Scientific Publishers, Oxford.
115. Page, C. C., Moser, C. C., Chen, X., and Dutton, P. L. (1999) *Nature 402*, 47−52.
116. Ponce, A., Gray, H. B., and Winkler, J. R. (2000) *J. Am. Chem. Soc. 122*, 8187−8191.
117. Marcus, R. A., and Sutin, N. (1985) *Biochim. Biophys. Acta 811*, 265−322.
118. Marcus, R. A. (1997) *Pure Appl. Chem. 69*, 13−29.
119. Faller, P., Pascal, A., and Rutherford, A. W. (2001) *Biochemistry 40*, 6431−6440.
120. Hanley, J., Deligiannakis, Y., Pascal, A., Faller, P., and Rutherford, A. W. (1999) *Biochemistry 38*, 8189−8195.
121. Tracewell, C. A., Cua, A., Stewart, D. H., Bocian, D. F., and Brudvig, G. W. (2001) *Biochemistry 40*, 193−203.
122. De Paula, J. C., Li, P. M., Miller, A.-F., Wu, B. W., and Brudvig, G. W. (1986) *Biochemistry 25*, 6487−6494.
123. Kaminskaya, O. P., and Shuvalov, V. A. (1994) *FEBS Lett. 355*, 301−304.
124. Wang, J., Gosztola, D., Ruffle, S. V., Hemann, C., Seibert, M., Wasielevski, M. R., Hille, R., Gustafson, T. L., and Sayre, R. T. (2002) *Proc. Natl. Acad. Sci. U.S.A. 99*, 4091−4096.

BI020606V